

## **THERMOGRAVIMETRIC DETERMINATIONS OF THE WATER SORPTION CHARACTERISTICS OF MOLECULAR SIEVE IN HIGH-PRESSURE CO<sub>2</sub> AND N<sub>2</sub>**

N.A. BURDETT

*Central Electricity Generating Board, Marchwood Engineering Laboratories, Marchwood, Southampton, SO4 4ZB (Gt. Britain)*

(Received 11 September 1984)

### **ABSTRACT**

The rates and extents of H<sub>2</sub>O adsorption by molecular sieves have been determined in order to assess the possibility of using these materials as desiccants in the driers on advanced gas cooled nuclear reactors. Microbalance experiments have been conducted on AW500 and 3A sieves at a sorption temperature of 35°C, using N<sub>2</sub> and CO<sub>2</sub> as carrier gases and at total pressures between 2 and 43 atm. Interpretation of the microbalance data is complicated by co-adsorption of carrier gas and water. The large differences in adsorption and desorption rates between the carrier gas and water (due to very large concentration driving forces for the mass transfer processes) allow quantification of the adsorption of both components using weight data only.

### **INTRODUCTION**

The coolant gas in an advanced gas cooled reactor (AGR) is primarily CO<sub>2</sub> although other gases, such as water vapour, are present in small amounts. Control of the moisture content is currently achieved by the use of driers filled with beads of silica gel. The moisture capacity of this desiccant is higher in air than under the 40 atm CO<sub>2</sub> pressure experienced in AGRs, indicating co-adsorption of the CO<sub>2</sub> [1]. The work reported here is part of a study initiated in order to ascertain whether molecular sieves had any potential for replacing the existing desiccant and involved the determination of the relevant sorption capacities and kinetics.

A thermogravimetric technique was used since it was more rapid than methods exploiting packed beds or similar systems. In addition, by careful calibration, etc., it proved possible to determine the magnitude of the co-adsorption problem, i.e., the reduction of water capacity due to adsorption of CO<sub>2</sub>.

## EXPERIMENTAL

*Apparatus*

The apparatus is shown in Fig. 1. It consists of a Sartorius ultramicrobalance capable of operating at the desired pressures (up to 45 atm) and an arrangement for controlling the flow and composition of gas passing over the reacting particles. Molecular sieve pellets were suspended in a quartz tray from one arm of the balance and the weight change monitored as a function of time as water vapour was adsorbed. Usually about six 1/16-in. pellets were used in order to produce a sufficiently large total weight change, although one 1/8-in. particle was found to be adequate. The pellets were cylindrical in cross-section and were truncated before reaction into a right-cylindrical shape. This process aids the interpretation of the data since the kinetic expressions describing diffusion in such systems are identical in form to those for a sphere. The mode of operation of the apparatus was as follows.

Carrier gas ( $\text{CO}_2$  or  $\text{N}_2$ ) was led from a cylinder into two desiccant beds (B1 and B2 in Fig. 1) containing high and low moisture loadings, respectively. Variations in the relative flows through these beds produced the desired water vapour concentration in the reaction gas. A supply of dry gas was taken from the outlet of the bed of regenerated desiccant (B2) and passed into the microbalance, the flows through each of the two arms of the balance being adjusted to the values required during the experiment. This procedure enabled the system to stabilise in dry gas at the correct reaction temperature ( $35^\circ\text{C}$ ) in order to determine an accurate initial weight reading and also to balance any aerodynamic effects of high flow rates. The temperature of the gas flowing past the pellets was adjusted to the desired

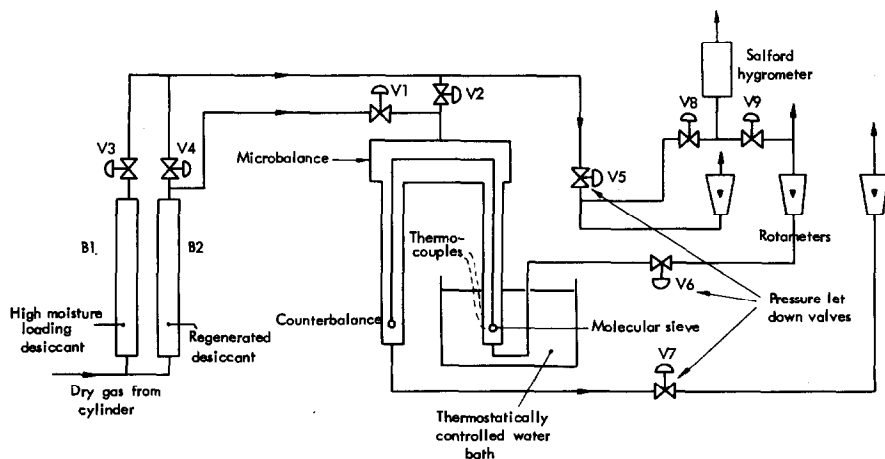


Fig. 1. Apparatus.

value by means of a thermostatically controlled water bath containing the lower parts of both balance arms.

The flows of gas through V3 and V4 were adjusted until the gas mixture contained the required H<sub>2</sub>O vapour concentration and the overall flow through V5 equalled the total flow of dry gas entering the microbalance via V1. On achieving stable conditions, V1 and V5 were closed and V2 opened allowing wet gas into the system at the correct rate. V5 was closed to ensure the correct gas flow rate through the microbalance.

The concentration of H<sub>2</sub>O in the gas entering and leaving the balance could be determined by passing a small flow (100 cm<sup>3</sup> min<sup>-1</sup>) from the main flow through a Salford hygrometer. A continuous record of [H<sub>2</sub>O] could therefore be obtained throughout the experiment. It was observed that, once set, the valves V3, V4 rarely required adjustment and, provided that the ambient temperature remained fairly constant, the amount of water vapour in the reactant gas did not vary much. Experiments were left running overnight, [H<sub>2</sub>O] not deviating by more than  $\pm 10\%$  during that period.

Regeneration of the molecular sieve was carried out in the microbalance at 40 atm, with a flow of carrier gas containing 300 vpm H<sub>2</sub>O passing over the pellets. The balance arm was heated by means of a vertical tube furnace and the system temperature allowed to rise slowly up to either 200 or 280°C. This temperature was maintained until there was no further change in the weight of the particles or in the water content of the gas flowing out of the balance. The apparatus was then filled with dry gas and simultaneously cooled down to the reaction temperature of 35°C.

### *Microbalance operation at high pressures*

Baseline characteristics of the microbalance are affected by experimental variables such as gas flow rate. Aerodynamic forces exert a drag on the particles and sampling basket in the measurement arm as well as on the counterbalance weights. Adjustment of the gas flows during operation balances the drag on each arm, so that the apparent weight of the particle is identical under static and flowing conditions. Provided that the experiment is conducted isothermally, no correction to the measured weight change is necessary. As the pressure in the system is increased, aerodynamic effects become less important since, at constant mass throughput, the velocity of the reaction gas is inversely proportional to gas pressure.

As the density of the gas surrounding the reacting material increases due to rising pressure, complications due to buoyancy become significant. Because of the small, inevitable, difference in volume between the two balance arms (denoted  $\Delta V$ ) there is a change of weight  $\Delta W_p$  given by

$$\Delta W_p = \Delta V \Delta \rho_p \quad (1)$$

where  $\Delta\rho_P$  is the change in gas density caused by the pressure variation. Figure 2 shows plots of the baseline against pressure for two empty quartz baskets of different size, both suspended in the measurement balance arm, the counterbalance and suspension wires being the same for both cases. It is evident firstly, that in one case  $\Delta V$  is negative and in the other positive, and secondly, that weighing in  $\text{CO}_2$  produces greater baseline shifts than weighing in  $\text{N}_2$ . Equation (1) shows that the ratio of the slopes of the plots for a basket suspended in air and  $\text{CO}_2$  is proportional to the relative densities of these two gases, or more simply to the ratio of their molecular weights. This is found to be the case for both examples shown in Fig. 2. In addition, the difference in volume between the two baskets tested should be given by the expression

$$\left[ \frac{\Delta W_P}{\Delta\rho_P} \right]_1 - \left[ \frac{\Delta W_P}{\Delta\rho_P} \right]_2 = (V_1 - V_2) \quad (2)$$

where  $V_1$  and  $V_2$  are the volumes of the two pieces of quartz. The validity of eqn. (2) may be verified by calculating the term  $(V_1 - V_2)$  through the weight difference and the known density of quartz glass, this being found to be  $0.0670 \text{ cm}^3$  compared with a value of  $0.0657 \text{ cm}^3$  from eqn. (2).

Because of the effects of buoyancy, a correction has to be applied to all measurements made on the microbalance at high pressure. The true weight change ( $W$ ) due to hydration/adsorption is related to the measured one

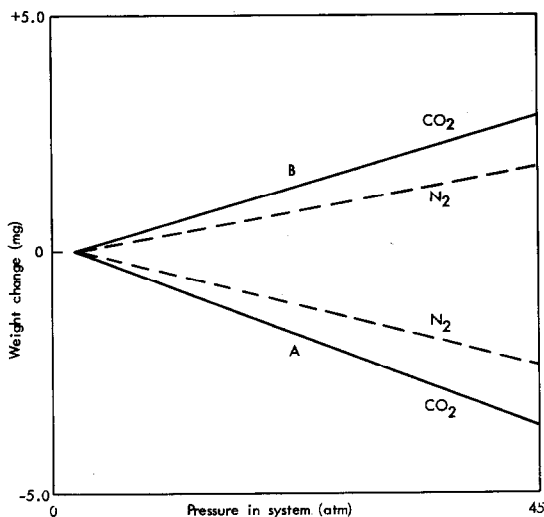


Fig. 2. Plots of baseline weight as a function of total pressure for two empty quartz baskets (A, B) weighed in  $\text{CO}_2$  and  $\text{N}_2$ .

( $W^*$ ) by the expression

$$W = W^* \left( 1 + \frac{\rho_g}{\rho_m} \right) \quad (3)$$

where  $\rho_g$  and  $\rho_m$  are the densities of the gas and particle, respectively, at the operational conditions of pressure and temperature. For the case of molecular sieve reacting at 35°C in 40 atm CO<sub>2</sub>, the correction is not very significant,  $W/W^*$  being about 1.06.

Raising the temperature of the system also produces a significant effect on the baseline of the microbalance. During regeneration of the molecular sieve, the furnace is placed around one side of the balance so the apparatus responds to changes in density in the measurement arm compared with the counterbalance arm. By analogy with eqn. (1)

$$\Delta W_T = \Delta V_T \Delta \rho_T \quad (4)$$

where  $\Delta V_T$  is the volume of the heated arm and  $\Delta \rho_T$  is the density change caused by the temperature variation. Since the density is reduced on increasing the temperature (proportional to  $T^{-1}$ ), it would be expected that raising the temperature would cause an increase in baseline weight. This was confirmed by experiments which showed that when six unhydrated pellets were subjected to a temperature rise from 35 to 280°C, a baseline weight change of around 6 mg could be detected. This is considerably more than the weight change resulting from the hydration, and it was therefore considered that any measurements of regeneration kinetics would be subject to large experimental errors.

## RESULTS

### *Adsorption of carrier gas*

The value of the microbalance in determining the rate of reaction as well as the ultimate hydration capacity of a molecular sieve particle depends largely on the attribution of an observed weight change to a single process. Consideration of the data presented here indicates that the hydration of the desiccant was accompanied by desorption of the carrier gas so that measured weight changes were inevitably lower than would otherwise be the case. An example of this is the hydration of 1/16-in. AW500 pellets (at 40 atm pressure, 35°C and with 300 vpm H<sub>2</sub>O), results being shown in Fig. 3. A significant weight change was obtained when an N<sub>2</sub> carrier gas was used, although with CO<sub>2</sub> only a small increase could be detected. In fact, it was noticed that there was an initial decrease in weight in the case of CO<sub>2</sub>, suggesting that adsorption of H<sub>2</sub>O displaced CO<sub>2</sub> from sites on the molecular sieve. The overall change in weight at the end of the 20-h experiment was

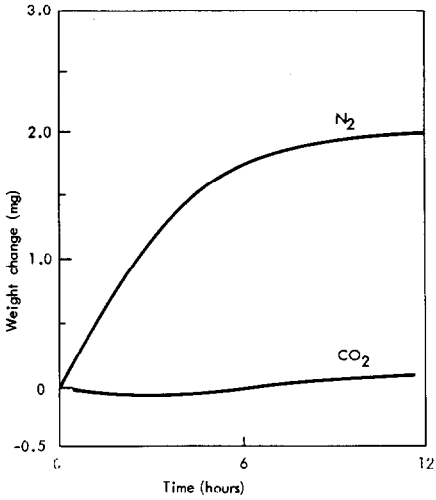


Fig. 3. Plots of measured weight change as a function of time for six 1/16-in. AW500 pellets reacted in 300 vpm H<sub>2</sub>O at 35°C in 40 atm N<sub>2</sub> or CO<sub>2</sub>.

minimal and hence estimates of the water capacity impossible. In order to confirm that the particles had in fact absorbed H<sub>2</sub>O, the gas stream emerging from the microbalance after passing over the particles was monitored during regeneration at 40 atm CO<sub>2</sub>, 300 vpm H<sub>2</sub>O, a temperature of

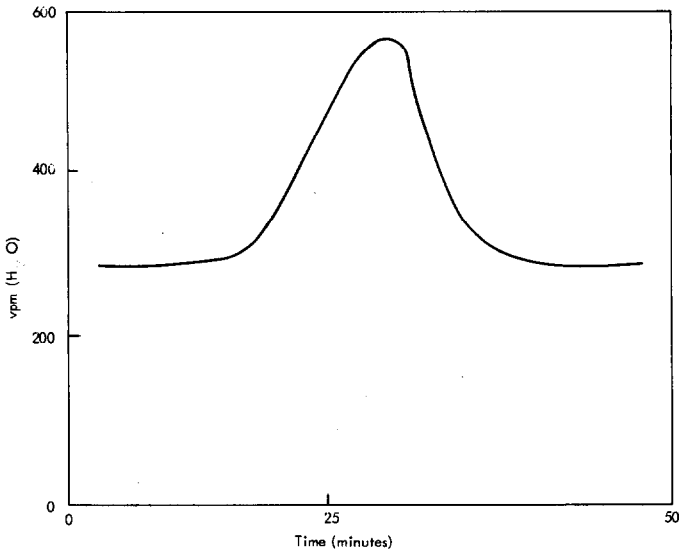


Fig. 4. Plot of water concentration in exit gas stream during regeneration of AW500 pellets in 300 vpm H<sub>2</sub>O, 40 atm CO<sub>2</sub>.

200°C being finally attained. Figure 4 shows a trace of the H<sub>2</sub>O concentration against time during this heating period; the particles being regenerated are those which showed no weight change in CO<sub>2</sub>. A significant quantity of water was driven off the sieve during heating, integration of the curve of Fig. 4, together with knowledge of overall gas flow rates, indicating that 1.96 mg was evolved. Even after allowing for errors in the determination, such as desorption of water from the stainless-steel pipework, it may be concluded that AW500 molecular sieve reacted with H<sub>2</sub>O vapour in CO<sub>2</sub> does absorb water but that displacement of CO<sub>2</sub> also occurs. Coincidentally, it appears that under these particular conditions the weight of water absorbed is approximately equal to the weight of CO<sub>2</sub> desorbed, yielding a zero overall weight change throughout the experiment.

Clearly, in order to calculate the extent of hydration from the observed weight changes, it is important to determine the extent of carrier gas desorption due to H<sub>2</sub>O adsorption. This was achieved by studying the weight increases caused by raising the pressure in the microbalance with molecular sieve pellets suspended on the quartz tray in the carrier gas. When step changes were made in the pressure in the system, the resulting variations in baseline weight were rapid and completely reversible. (This is in complete contrast to the hydration process which, under the conditions employed here, is slow and effectively irreversible). In addition, the extent of baseline shift was found to be dependent on the dryness of the particle (i.e., before or after regeneration). Figure 5 shows typical data for the magnitude of the apparent weight changes plotted against system pressure for some 1/16-in. 3A pellets weighed in both dry CO<sub>2</sub> and dry N<sub>2</sub> before and immediately

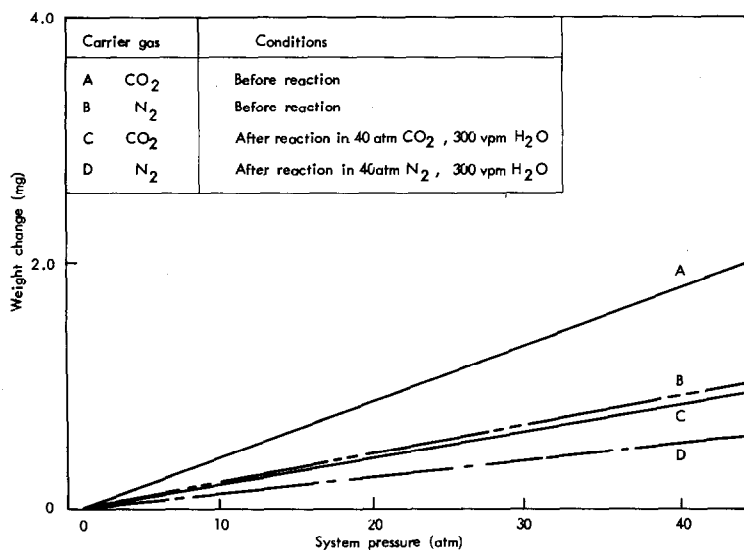


Fig. 5. Plot of weight changes for six 1/16-in. 3A pellets as a function of system pressure.

after hydration. Using the assumptions that carrier gas adsorption is rapid and reversible, whereas hydration is irreversible and relatively slow, it is possible to equate the difference in baseline weights between wet and dry pellets to the extent of carrier gas desorption during hydration. By a similar argument, it is possible to estimate the absolute magnitude of the carrier gas adsorption by comparing the change in baseline when pellets are subjected to an increase in pressure to that calculated from their known volume and the theoretical buoyancy correction using eqn. (1). It was thus possible to estimate the extent of adsorption of  $\text{CO}_2$  and  $\text{N}_2$  from the baseline variation as the pressure was altered and this was found to vary with the dryness of the particle (i.e., either before or after regeneration). Table 1 sets out typical fractional adsorptions of  $\text{CO}_2$  and  $\text{N}_2$  by AW500 and 3A molecular sieves when regenerated at  $200^\circ\text{C}$  and 40 atm in 300 vpm  $\text{H}_2\text{O}$  and after reaction at or around 40 atm in 300 vpm  $\text{H}_2\text{O}$  at  $35^\circ\text{C}$ .

In the case of AW500 sieve reacted with  $\text{H}_2\text{O}$  in  $\text{CO}_2$ , the observation that no weight change occurred even though the particle hydrated suggests that the weight of  $\text{H}_2\text{O}$  adsorbed equalled the weight of  $\text{CO}_2$  desorbed. This in turn suggests that 1 molecule of  $\text{CO}_2$  was displaced by nearly  $2\frac{1}{2}$  molecules of  $\text{H}_2\text{O}$  on this material. From the data given in Table 1 this fact may be utilised to suggest that the hydration capacity of this material is about 9%. For 3A sieve, however, 5.7 molecules of  $\text{H}_2\text{O}$  were required to displace one  $\text{CO}_2$ , which suggests that competition for available sites is not so severe with this material as for AW500, this conclusion being compatible with the relative pore diameters of the two molecular sieves.

#### *Equilibrium capacity of molecular sieves*

The adsorption capacity of the molecular sieves under the experimental conditions of the microbalance are shown (after correction for buoyancy and co-adsorption) in Fig. 6 where the data are plotted as the equilibrium

TABLE 1

Capacities of AW500 and 3A molecular sieves for  $\text{N}_2$ ,  $\text{CO}_2$  at 40 atm,  $35^\circ\text{C}$

Sieve	State	Carrier gas	Wt. carrier gas (g) per g sieve
AW500	wet	$\text{CO}_2$	0.10
	dry	$\text{CO}_2$	0.19
	wet	$\text{N}_2$	0.006
	dry	$\text{N}_2$	0.012
3A	wet	$\text{CO}_2$	0.006
	dry	$\text{CO}_2$	0.05
	wet	$\text{N}_2$	0
	dry	$\text{N}_2$	0.007



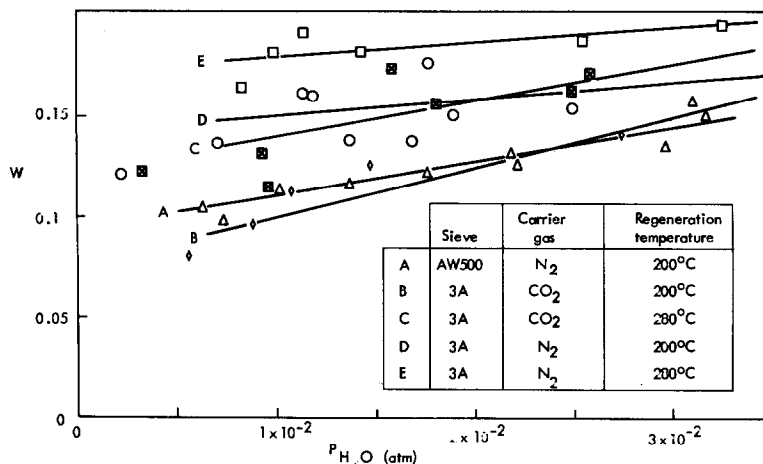


Fig. 6. Plots of measured H<sub>2</sub>O uptake against the partial pressure of H<sub>2</sub>O.

loading against water concentration. It is clear from this diagram that, for the majority of the results, the loading is not very sensitive to the H<sub>2</sub>O partial pressure; i.e., the part of the isotherm under investigation is nearly flat. In consequence, the derivation of the characteristics of the isotherm is not likely to be particularly accurate. However, on the assumption that the hydration of molecular sieves under the experimental conditions follows a Langmuir isotherm, then the amount of H<sub>2</sub>O adsorbed ( $W$ ) may be described by the expression

$$\frac{W_{\max}}{W} = 1 + \frac{B}{P_{\text{H}_2\text{O}}} \quad (5)$$

where  $W_{\max}$  is the maximum water loading,  $B$  is a constant and  $P_{\text{H}_2\text{O}}$  the partial pressure of H<sub>2</sub>O in the ambient gas.

For the situation under consideration here, it is impossible to completely regenerate the material by heating to 200 or 280°C in 300 vpm H<sub>2</sub>O, and hence  $W_{\max}$  represents the maximum amount of H<sub>2</sub>O which may be adsorbed and desorbed by the sieve under the particular regeneration conditions employed. Manipulation of eqn. (5) suggests that a plot of  $1/W$  against  $1/P_{\text{H}_2\text{O}}$  should yield a line from which the constants  $W_{\max}$  and  $B$  may be readily obtained, approximate values of these constants being tabulated in Table 2.

### Kinetic analysis

The data obtained in this study have been analysed in order to ascertain the rate of water sorption and hence the diffusional parameters associated with the molecular sieve. It was assumed that the hydration kinetics were

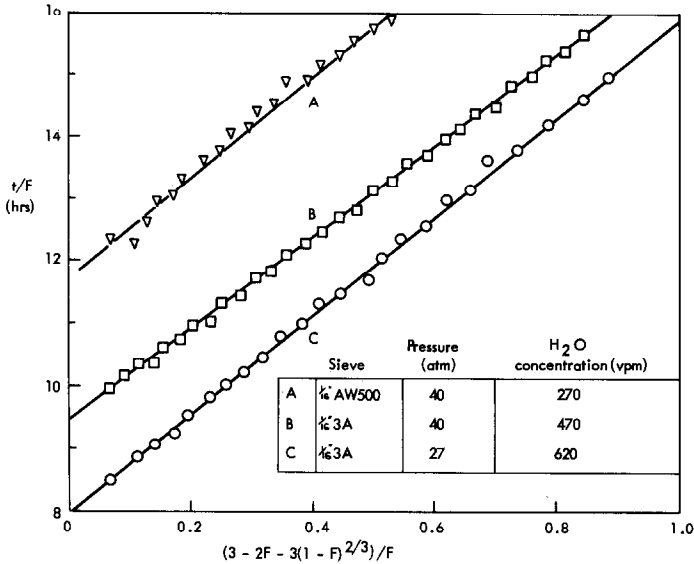


Fig. 7. Typical plots of  $t/F$  against  $[3 - 2F - 3(1 - F)^{2/3}]/F$  (from eqn. 6).

controlled by two factors, the rate of mass transfer of H<sub>2</sub>O across the solid/gas boundary layer and the rate of its diffusion into the porous particle. Using a quasi-steady state approach and the approximation of the shrinking-core model, it may be shown [2] that the rate expression may be given by

$$\frac{4\pi R^2 C_0 t}{\Delta M F} = \frac{1}{kg} + \frac{R}{2D_s F} [3 - 2F - 3(1 - F)^{2/3}] \quad (6)$$

where  $R$  is the particle radius,  $C_0$  the bulk gas H<sub>2</sub>O concentration,  $\Delta M$  the equilibrium H<sub>2</sub>O loading,  $t$  the time,  $kg$  a mass-transfer coefficient,  $D_s$  the effective diffusion coefficient and  $F$  the fractional conversion. Figure 7

TABLE 2  
Molecular sieve capacities for H<sub>2</sub>O

Sieve	Carrier gas	Regeneration temp. (°C)	$W_{\max}^a$	$B^a$ (atm)	Capacity at 40 atm/300 vpm H <sub>2</sub> O (g H <sub>2</sub> O/g sieve)
AW500	N <sub>2</sub>	200	0.17	$5.2 \times 10^{-3}$	0.124
3A	N <sub>2</sub>	200	0.18	$2.0 \times 10^{-3}$	0.151
		282	0.21	$1.9 \times 10^{-3}$	0.185
	CO <sub>2</sub>	200	0.17	$6.0 \times 10^{-3}$	0.116
		282	0.20	$4.5 \times 10^{-2}$	0.197

<sup>a</sup>  $W_{\max}$  and  $B$  are constants in Langmuir adsorption isotherm (eqn. 5).

shows plots of  $t/F$  against  $[3 - 2F - 3(1 - F)^{2/3}]/F$ , inspection of eqn. (6) indicating that  $kg$  and  $D_s$  may be easily derived from the intercept and slope of the resulting straight line. For all the experiments conducted here, the linearity of the plots was excellent, deviations only becoming noticeable at  $F > 0.85-0.9$ , where errors in determining  $F$  become evident due to the slowness of the adsorption at this point. For all these data, the values of weight increase must be corrected as explained earlier to account for the effects of co-adsorption of the carrier gas and of buoyancy. These can be significant, for example, an adsorption in 300 vpm  $H_2O$  at 40 bar requires correction factors of 1.13 and 1.43 for hydration in  $N_2$  and  $CO_2$ , respectively.

For the systems studied here, the effective diffusion coefficient ( $D_s$ ) is a combination of Knudsen and bulk diffusion coefficients ( $D_K$  and  $D_B$ , respectively). Satterfield and Sherwood [3] use an approximation for  $D_s$ , i.e.

$$\frac{1}{D_s} = \frac{1}{D_B} + \frac{1}{D_K} \quad (7)$$

or (since  $D_B$  is inversely dependent on pressure)

$$\frac{1}{D_s} = \frac{1}{D_K} + P\lambda \quad (8)$$

where  $\lambda$  is a constant. Figure 8 shows plots of  $D_s^{-1}$  against  $P$  for all the data collected in these experiments, the intercept being related to  $D_K$  and the slope equal to  $\lambda$ . Discussion of the magnitudes of the relevant diffusion coefficients is unnecessary here, it is sufficient to state that they are in line with other similar determinations (e.g., Nutter and Burnett [4]) and hence that the thermogravimetric technique is capable of generating reproducible results.

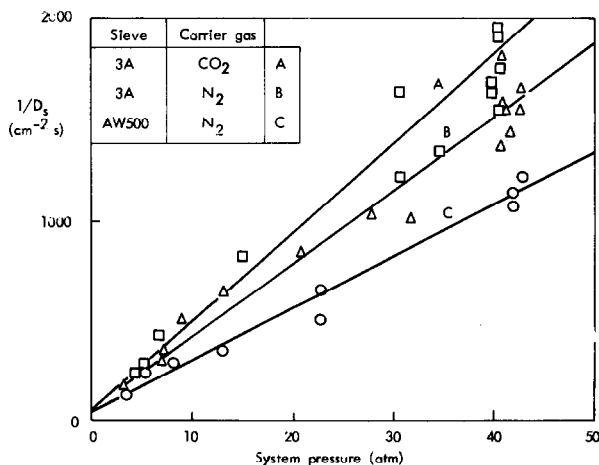


Fig. 8. Plots of reciprocal of diffusion coefficient,  $D$ , against system pressure.

## ACKNOWLEDGEMENT

This work was performed at the Marchwood Engineering Laboratories and is published by permission of the Central Electricity Generating Board.

## REFERENCES

- 1 B.H.M. Billinge and R.E. Streatfield, Conf. on Gas Chemistry in Nuclear Reactor and Large Industrial Plant, Salford, 1980.
- 2 N.A. Burdett, B.J. Gliddon and R.C. Hotchkiss, Combust. Sci. Technol., 27 (1980) 107.
- 3 C.N. Satterfield and T.K. Sherwood, The Role of Diffusion in Catalysis, Addison Wesley, New York, 1967.
- 4 J. Nutter and C. Burnett, Ind. Eng. Chem., Proc. Des. Dev., 5 (1966) 1.